The EMBO Journal vol.14 no.14 pp.3373–3384, 1995

The *Drosophila* insulin receptor homolog: a gene essential for embryonic development encodes two receptor isoforms with different signaling potential

Rafael Fernandez[1,2], Diane Tabarini[2], Natalia Azpiazu[3], Manfred Frasch[3] and Joseph Schlessinger[1,4]

[1]Department of Pharmacology, New York University Medical Center, 550 First Avenue, New York, NY 10016, [2]Program in Molecular Biology, Memorial Sloan Kettering Cancer Center, New York and [3]Brookdale Center for Molecular Biology, Mount Sinai School of Medicine, New York, NY, USA

[4]Corresponding author

We report the cloning and primary structure of the *Drosophila* insulin receptor gene (*inr*), functional expression of the predicted polypeptide, and the isolation of mutations in the *inr* locus. Our data indicate that the structure and processing of the *Drosophila* insulin proreceptor are somewhat different from those of the mammalian insulin and IGF 1 receptor precursors. The INR proreceptor (M_r 280 kDa) is processed proteolytically to generate an insulin-binding α subunit (M_r 120 kDa) and a β subunit (M_r 170 kDa) with protein tyrosine kinase domain. The INR β_{170} subunit contains a novel domain at the carboxy-terminal side of the tyrosine kinase, in the form of a 60 kDa extension which contains multiple potential tyrosine autophosphorylation sites. This 60 kDa C-terminal domain undergoes cell-specific proteolytic cleavage which leads to the generation of a total of four polypeptides (α_{120}, β_{170}, β_{90} and a free 60 kDa C-terminus) from the *inr* gene. These subunits assemble into mature INR receptors with the structures $\alpha_2(\beta_{170})_2$ or $\alpha_2(\beta_{90})_2$. Mammalian insulin stimulates tyrosine phosphorylation of both types of β subunits, which in turn allows the β_{170}, but not the β_{90} subunit, to bind directly to p85 SH2 domains of PI-3 kinase. It is likely that the two different isoforms of INR have different signaling potentials. Finally, we show that loss of function mutations in the *inr* gene, induced by either a P-element insertion occurring within the predicted ORF, or by ethylmethane sulfonate treatment, render pleiotropic recessive phenotypes that lead to embryonic lethality. The activity of *inr* appears to be required in the embryonic epidermis and nervous system among others, since development of the cuticle, as well as the peripheral and central nervous systems are affected by *inr* mutations.

Key words: *Drosophila melanogaster*/insulin receptor/IRS-1/nervous system development/tyrosine kinase

Introduction

Insulin is best known for its essential role in stimulating metabolic processes such as glucose uptake as well as glycogen and fatty acids synthesis (Kahn, 1994). However, insulin can also act as a mitogen for fibroblasts and other cell types in culture. Insulin mediates its biological responses by binding to, and activating, a heterotetrameric, cell-surface receptor termed the insulin receptor (reviewed by White and Kahn, 1994). A major cellular protein that is phosphorylated on numerous tyrosine residues in response to insulin stimulation is the insulin receptor substrate 1 (IRS-1, White *et al.*, 1985). It has been shown that different tyrosine phosphorylation sites on IRS-1 serve as binding sites for a variety of SH2 domains (Pawson and Schlessinger, 1993) of signaling molecules including phosphatidyl-inositol-3 kinase (PI-3K), Grb2, Nck and Syp (Keller and Lienhard, 1994; Myers *et al.*, 1994a). In addition, insulin stimulates tyrosine phosphorylation of the adaptor protein Shc. Tyrosine phosphorylated Shc binds Grb2–Sos complex leading to the activation of the Ras/MAP kinase signaling pathway, which constitutes an alternative mechanism to the IRS-1 mediated activation of the Ras/MAPK signaling pathway (Skolnik *et al.*, 1993).

The ability of insulin and insulin-like growth factors (IGFs) 1 and 2, which activate the IGF 1 receptor (Ullrich *et al.*, 1986), to act as both mitogens and differentiation factors has been shown to be dependent on activation of the Ras/MAP kinase signaling cascade. These responses can be mimicked by activated forms of Ras, and blocked by a dominant negative Ras mutant (Benito *et al.*, 1991; Porras *et al.*, 1992). However, recent studies have suggested that some of the metabolic responses triggered by insulin, such as stimulation of glucose transport in adipocytes mediated by the insulin-sensitive glucose transporter GLUT4, are independent of Raf or Ras stimulation (Fingar and Birnbaum, 1994; Hausdorff *et al.*, 1994). Furthermore, stimulation of the Ras signaling pathway by EGF in 3T3-L1 adipocytes does not promote GLUT4 translocation to the plasma membrane and glucose uptake, or the stimulation of glycogen synthesis (Robinson *et al.*, 1993; Fingar and Birnbaum, 1994). Recent studies with inhibitors of PI-3K, or overexpression of PDGF receptor mutants that fail to activate PI-3K, have suggested that stimulation of PI-3K is required for stimulation of the rapamycin-sensitive p70-S6 kinase (Cheatham *et al.*, 1994; Chung *et al.*, 1994; Ming *et al.*, 1994). Activation of the p70-S6 kinase itself has been shown to be dispensable for the insulin-stimulated GLUT4 translocation (Fingar *et al.*, 1993); however, it is thought that this process still requires activation of PI-3K (Cheatham *et al.*, 1994). This suggests that PI-3K activates multiple downstream targets (Cheatham *et al.*, 1994; Myers *et al.*, 1994b).

To understand the biological significance of the pleiotropic effects of insulin on metabolic processes as well as on cell growth and differentiation, we have undertaken a reverse genetic approach by cloning *Drosophila* homologs of the insulin signaling pathways. Here we report the

cloning and expression of the gene encoding the *Drosophila* insulin receptor, and the isolation of mutant alleles in the *inr* locus. Unlike mammalian insulin and IGF 1 receptors, INR contains a large extension at the C-terminus that may serve as binding site for SH2 containing signaling molecules. Our findings suggest that the basic mechanisms of signaling utilized by insulin have been conserved in *Drosophila*. Therefore, the minimal framework necessary for activation of multiple signaling cascades leading to a variety of effects in mammalian systems, is also present and presumably utilized in a similar fashion in *Drosophila*.

Results and discussion

The inr gene encodes an insulin receptor-like precursor with a large carboxy-terminal extension

The *Drosophila* insulin receptor homolog (*inr*, according to Lindsley and Zimm, 1992) was cloned by low stringency hybridization to a human insulin receptor (HIR) cDNA probe (Petruzzelli *et al.*, 1986). The isolation and sequencing of overlapping genomic and cDNA clones covering all of the coding region of the INR gene, as well as the mapping of the major INR transcriptional unit (see details in Figure 1A), allowed us to identify an ORF (Figure 1B) which based on its overall organization and predicted topology, seemed to encode an insulin receptor-like preproreceptor polypeptide. The INR ORF is highlighted by the conservation of the potential insulin-binding and tyrosine kinase domains, as well as the location of a furin-like site for proteolytic processing that specifies the cleavage of the α from the β subunit, and a transmembrane domain preceding the tyrosine kinase domain (Figures 1 and 2). The highest degree of sequence identity in the extracellular domain (~39%) is centered around the most N-terminal 450 amino acids (from residues 38 to 480 of the HIR sequence, alignment shown in Figure 2B). This corresponds to the domains thought to be responsible for high-affinity binding of insulin and IGF 1 (Zhang and Roth, 1991; Andersen *et al.*, 1992; Fabry *et al.*, 1992). Two stretches of 130–140 amino acid residues flanking the single cysteine-rich domain are thought to be responsible for high-affinity binding of insulin (reviewed by De Meyts, 1994; Schäffer, 1994), whereas the cysteine-rich domain itself appears to possess sequences that determine high-affinity binding for IGF-1 (Schumacher *et al.*, 1991; Zhang and Roth, 1991). Although previous biochemical studies indicated that INR shows preferential binding to mammalian insulin over IGF-1 (Petruzzelli *et al.*, 1985; Fernandez-Almonacid and Rosen, 1987), sequence alignment of these domains of INR with corresponding regions of the human insulin or IGF-1 receptors fail to show preferential homology toward either receptor. This suggests that only a few residues, or very short stretches of sequence within an overall similar architecture, may be responsible for determining preferential ligand binding.

An unusual feature found in the INR precursor was the presence of long extensions in the ORF, towards both the N- and the C-terminus (Figure 2A). Given the known topology of HIR, and biochemical data suggesting a similar topology for INR (Fernandez-Almonacid and Rosen, 1987; Fernandez-Almonacid, 1992), a possible explanation for the N-terminal extension was that the INR precursor undergoes membrane insertion via an internal signal peptide. Although uncommon, at least two other *Drosophila* proteins, the transmembrane Sevenless receptor (Bowtell *et al.*, 1988) and the secreted Hedgehog morphogen (Lee *et al.*, 1992), have been shown to have sequences indicative of internal signal peptides or type II membrane-anchoring domains. Alignment of the most N-terminal sequences of the human and *Drosophila* α subunits (Figure 2) shows that the homology starts four residues down from the human signal sequence cleavage site (Ebina *et al.*, 1985; Ullrich *et al.*, 1985). As expected, the *Drosophila* sequence is also preceded by a highly hydrophobic stretch. However, this potential signal sequence is located 43 residues upstream from the first amino acid matching the human sequence and, unlike most proreceptor sequences, it is not preceded by an initiator methionine. Rather, the most likely start site (Cavener and Ray, 1991) is located 223 codons upstream from the predicted first hydrophobic segment. We have accumulated evidence for functionality of both the initiator methionine and the signal sequence by transfection assays. We generated an expression vector that directs the synthesis of full-length INR (Figure 3), as well as internal deletion mutants that remove from amino acid residues 50–1500 or 310–1000, producing a soluble cytosolic C-terminus, and a membrane-anchored constitutively activated INR tyrosine kinase, respectively (data not shown).

The most remarkable conservation in the INR ORF falls in the region encoding the tyrosine kinase domain. The sequence surrounding tyrosine 1150 (numbering according to Ullrich *et al.*, 1985), YETDYY, containing the primary sites of autophosphorylation of the HIR kinase, which are also responsible for its autoactivation, is perfectly conserved (White and Kahn, 1994). Thus, the presence of all three tyrosines regarded as necessary for autoactivation of the kinase (Wilden *et al.*, 1992) predict a similar mechanism of autophosphorylation and activation for INR. A notably divergent motif of the INR kinase is the presence of a 20-amino acid kinase insert containing two tyrosine residues, while the HIR kinase has a small kinase insert that consists of only nine amino acids and lacks tyrosine residues. It is possible that the INR kinase insert becomes phosphorylated and is utilized as a docking site for SH2-containing proteins similarly to other growth factor receptors (Pawson and Schlessinger, 1993).

Two functions have been attributed to the juxtamembrane domain of HIR. Phosphorylation of Tyr960 has been implicated in the ligand-induced receptor internalization (Backer *et al.*, 1992) and tyrosine phosphorylation of IRS-1 (White *et al.*, 1988; reviewed by Myers *et al.*, 1994a) and Shc (Yonezawa *et al.*, 1994). It was recently shown that a domain of IRS-1 binds directly to the pTyr960 motif (O'Neill *et al.*, 1994). The juxtamembrane region of INR shows only a 23% sequence identity to the equivalent region in HIR. However, the high conservation of amino acid residues surrounding Tyr1306 makes this tyrosine a likely candidate for a Tyr960 equivalent in INR (VNPF **Y** ASMQ). Although we have not detected by biochemical methods an IRS-1 like molecule in *Drosophila* cell lines, as defined by White *et al.* (1985), the cloning of a conserved Shc-like molecule in *Drosophila* has been recently reported (Ka-Man *et al.*, 1994). Expression studies of human–*Drosophila* chimeric receptors that carry the entire *Drosophila* cytoplasmic indicate that Tyr1306 could

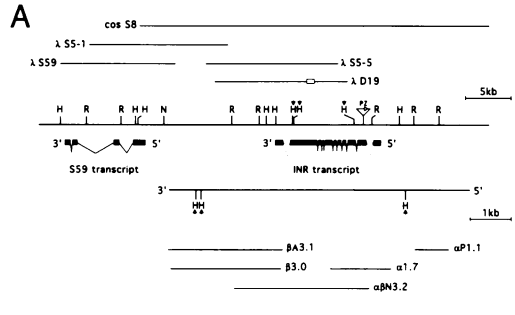

Fig. 1. Genomic walk around the *inr* locus and sequence of the major INR embryonic cDNA. (**A**) Restriction map (*Eco*RI, *Hin*dIII and *Not*I) of a 60 kb genomic walk around the cytological region 93E2-4 derived from partially overlapping phage and cosmid clones is shown on top. The genomic restriction map was derived from overlapping, independent genomic walks started from the S59 homeobox-containing gene (Dohrmann *et al.*, 1990) and from the tyrosine kinase domain of INR, shown by the open box on clone INRλ19 (Petruzzelli *et al.*, 1986). Shown at the bottom (at a larger scale) are overlapping INR cDNAs. A single 1.7 kb cDNA clone (α1.7) containing only α subunit-like sequences, and a 3.0 and a 3.1 kb cDNA clones (β3.0 and βA3.1), containing only β subunit-like sequences, were isolated from two embryonic cDNA libraries (Poole *et al.*, 1985). These clones, along with an independently isolated cDNA (αβN3.2) containing both α and β subunit sequences (Nishida *et al.*, 1986) were mapped to a single 12 kb *Eco*RI genomic fragment located 12 kb upstream from the S59 gene. Alignment (as indicated by arrowheads on top and under equivalent *Hin*dIII sites of genomic and cDNA clones) and orientation of the transcriptional units, based on Southern blotting and direct sequencing of genomic fragments, is also presented. The precise boundaries of the most 5′ and 3′ end exons were not mapped. Thus, only an approximate location (dotted lines) of the introns is shown. The insertion site of a transposable P-element (PZ, Karpen and Spradling, 1992), the recessive lethal insertion 3-5545 that is allelic to *inr* (obtained from T.Laverty), is shown at the 5′ end of the INR ORF (triangle). (**B**) The DNA sequence and conceptual translation of the longest ORF of the major INR embryonic transcript. The nucleotide sequence shown is a composite of genomic and cDNA sequences and corresponds to the entire coding region along with the entire 3′ untranslated region of the only poly(A) containing inr cDNA that was isolated (βA3.0). All cDNA clones shown in (A), with the exception of αβN3.2, were sequenced on both strands. To confirm the structure of the cDNA and to determine the exon/intron structure, we also sequenced subclones spanning the most 5′ 8 kb of the 12 kb *Eco*RI genomic fragment. The precise site of insertion of the PZ element, line 3-5545, is indicated by an arrow. The translational start site (underlined nucleotides 178–186) was assigned according to Cavener and Ray (1991), and represents three out of four matches (AGAA ATG) of the consensus *Drosophila* sequence for initiation of translation (C/A AA C/A ATG). This methionine was also used to drive overexpression of the INR protein from a minigene construct (see Materials and methods). The sequence preceding the translational start site (in italics) was derived from a genomic clone, and even though it contains four in-frame upstream methionines, it also has a consensus 3′ splice site (Mount *et al.*, 1992) seven nucleotides upstream from the initiator methionine chosen. The underlined nucleotide sequence at position 7117–7123 shows a consensus site for polyadenylation. Boxes surrounding amino acid sequences 223–240 and 1264–1287 represent the potential signal peptide and the transmembrane domain, respectively. Prediction of the signal peptide cleavage site was by the method of von Heijne (1986). This algorithm gives Ala243 a score of 10.88, a much higher value than the average score (3.5) for bona fide signal sequences (Lee *et al.*, 1992). The potential proteolytic processing site that generates α and β subunits of the mature receptor is shown at position 1036. Tyrosine residues 1917, 1941, 1957 and 1978, which may function as potential autophosphorylation/SH2 binding sites are shown by boxes.

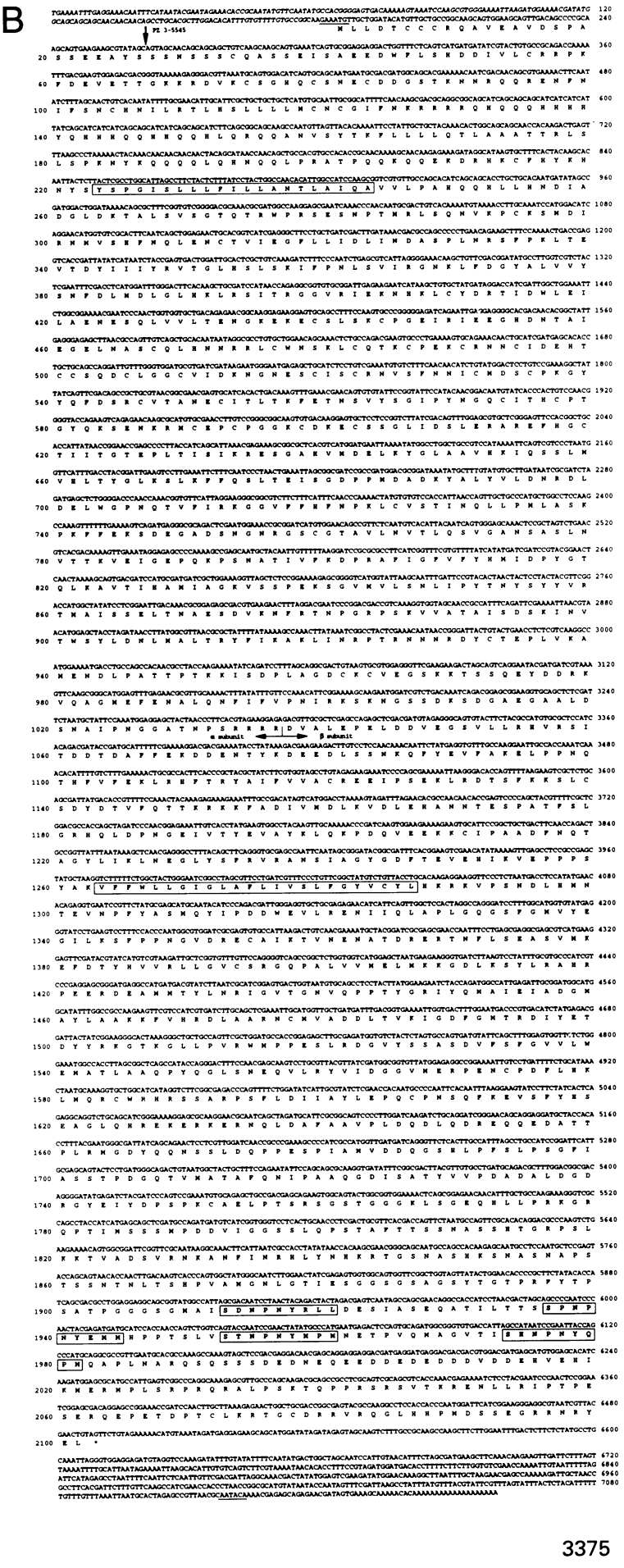

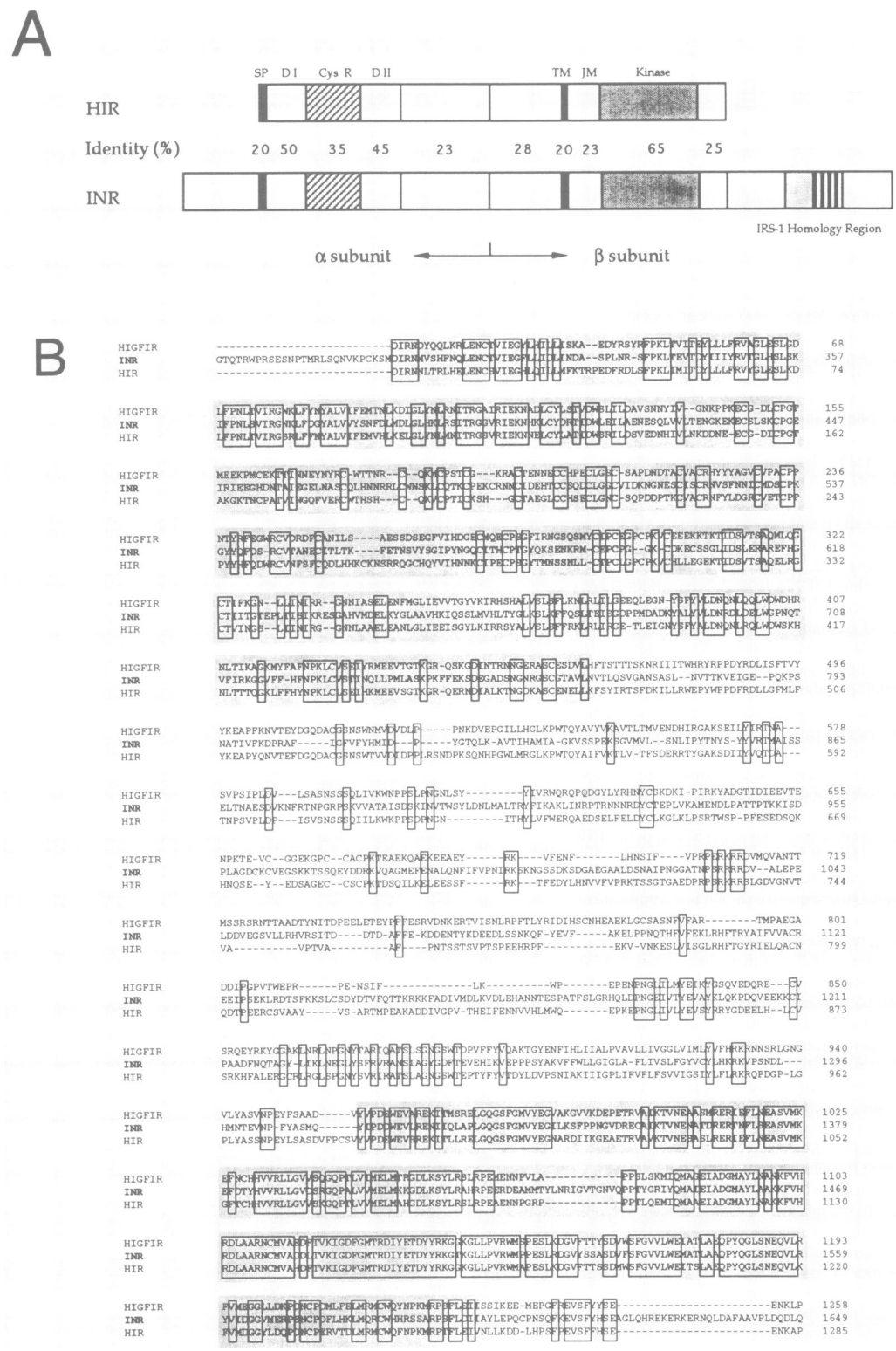

Fig. 2. Alignment of the *Drosophila* insulin receptor protein sequence with the human insulin and IGF 1 receptor sequences. A schematic representation of the homology between the *Drosophila* (INR) and the human insulin receptors (HIR), as well as the region of homology between the *Drosophila* insulin receptor C-terminal extension and the human IRS-1 protein (covering 150 amino acids that show 20% identity, indicated by four vertical bars) is shown in (**A**). The percentage of sequence identity of each independent domain of the HIR and INR sequences is shown. From the amino- to the carboxy-terminus the abbreviations used are: SP, signal peptide; DI, potential insulin-binding domain I; Cys R, cysteine-rich domain; DII, potential insulin-binding domain II; TM, transmembrane domain; JM, juxtamembrane region. In (**B**), the deduced amino acid sequences corresponding to the human insulin (HIR, Ebina *et al.*, 1985), human IGF 1 (HIGFIR, Ullrich *et al.*, 1986), and the *Drosophila* insulin (INR) receptors were aligned with the Geneworks 2.3 sequence analysis software package from Intelligenetics. Numbering of HIR and HIGFIR correspond to the mature receptors, whereas the INR numbers are from the proreceptor ORF. Boxes represent identical residues, and the shaded regions highlight the most strongly conserved regions: the putative ligand binding and the tyrosine kinase domains.

be phosphorylated in intact cells. These experiments show that INR readily phosphorylates IRS-1 and Shc in fibroblasts (Yamaguchi *et al.*, 1995) as well as Shc in the myeloid precursor 32 D cell line which lacks IRS-1 (L.Yenush *et al.*, manuscript in preparation).

The major difference between the mammalian and the *Drosophila* insulin receptors is the presence of a much larger carboxy-terminal tail in the *Drosophila* homolog. Nishida *et al.* (1986) reported the sequence of an embryonic cDNA (clone αβN3.2 in Figure 1A) that contained a stop codon following the subdomain XI of the kinase, at a position equivalent to Pro1705 of our sequence. However, we found a continuous ORF extending for 396 codons downstream from Pro1705. This was confirmed by sequencing four independent cDNA clones and two different genomic clones. The ORF of the carboxy-terminal tail contains several tyrosine residues, which seem to function as autophosphorylation sites. There appear to be at least four potential tyrosine phosphorylation sites in the INR carboxy-terminal tail (Figure 1B). These sites are characterized by the presence of five conserved amino acids N-terminal to the tyrosine (SXNPN Y) and by a variable sequence C-terminal to the tyrosine that may function as binding sites for SH2 domains of signaling proteins (Pawson and Schlessinger, 1993). Three of these tyrosines possess methionine residues in position +3 (YXXM), two of them being YMXM, which fits the consensus binding site for the SH2 domain of the p85 regulatory subunit of PI-3 kinase (Kapeller and Cantley, 1994). The tandem array of YXXM motifs spaced by ~14 residues spans a sequence region of ~140 amino acids, and shows a 20% sequence identity to a region in the N-terminal portion (residues 400–550) of IRS-1 (Sun *et al.*, 1991). It is now well established that in mammalian cells insulin recruits and activates PI-3 kinase by tyrosine phosphorylation of IRS-1 (White and Kahn, 1994). The presence of the C-terminal tail in INR could potentially allow it to carry out a similar process directly. Insulin could stimulate autophosphorylation of INR, and promote direct binding/activation of a *Drosophila* PI-3 kinase homolog, as well as the binding of other SH2-containing signaling proteins. As noted before, an additional feature of the potential phosphorylation sites of the INR carboxy terminal tail is the presence of the SXNPNY motifs. A similar sequence (LXNPXpY) was recently shown to be responsible for high-affinity binding of Shc, via its phosphotyrosine interaction domain (PID, Bork and Margolis, 1995) to the EGF receptor (A.G.Batzer *et al.*, submitted) and the polyoma middle T antigen (K.S.Campbell *et al.*, 1994).

A single INR precursor is differentially processed into two forms of mature INR receptors

Our previous biochemical characterization of the *Drosophila* insulin receptor indicated that it contained two different forms of both β (90 and 170 kDa), as well as α (110 and 120 kDa) subunits, and that these receptors

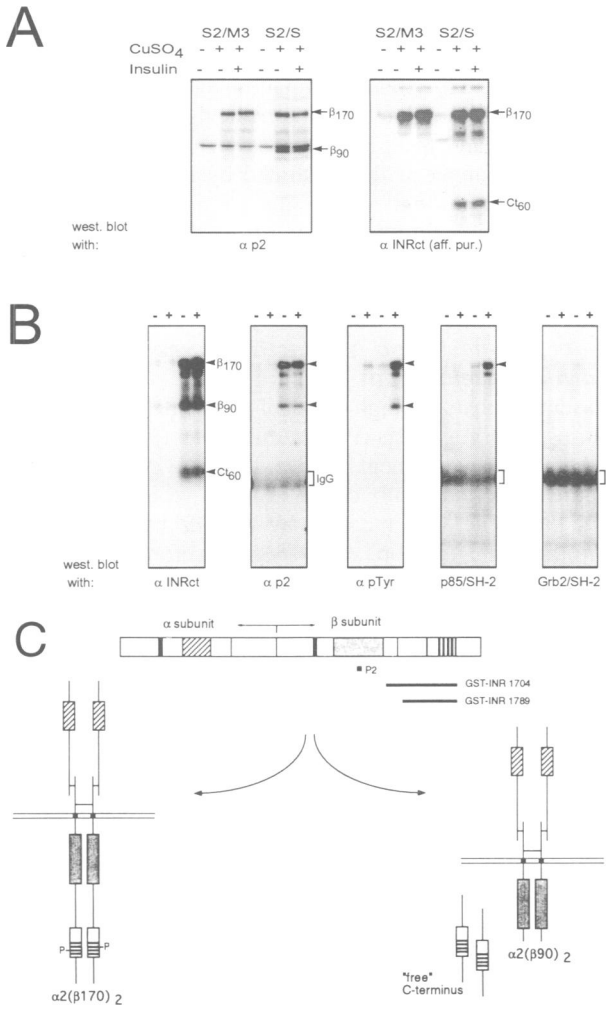

Fig. 3. Overexpression, differential processing and insulin-stimulated tyrosine phosphorylation of an *inr* minigene transfected in *Drosophila* cell lines. (**A**) Cell-specific, differential proteolytic processing of the INR β subunit, upon transient transfection in different *Drosophila* cell lines. Triton X-100 cell lysates (~20 μg of protein per lane) from cells transiently transfected (either S2/M3 or S2/S) with a *inr* minigene expression construct under control of the metallothionein promoter, either uninduced (–) or induced (+) with 0.7 mM $CuSO_4$, and either unstimulated (–) or stimulated (+) with 0.2 μM insulin for 90 min, were separated by SDS–PAGE (8% gel) and electroblotted onto nitrocellulose. Blots were probed with anti-INR antibodies, either anti-P2 (αp2) or anti-INR C-terminal that recognizes from residue 1789 to 1997 of INR (αINRct aff. pur.) antisera. (**B**) Insulin-stimulated tyrosine phosphorylation of INR in stably transfected *Drosophila* S2/S cells. Parental S2/S (left two lanes) or stably transfected cells overexpressing INR (right two lanes), obtained by co-transfection of pRmHa-INR with pPC4 (Jokerst *et al.*, 1989) and selection with α-amanitin, were induced with 0.7 mM $CuSO_4$ for 30 h, and either left quiescent (–), or stimulated (+) with 0.2 μM insulin for 10 min. Triton lysates prepared from these cells were immunoprecipitated with anti-INR C-terminal whole serum. The immunocomplexes were separated by SDS–PAGE (7% gel), and blotted onto nitrocellulose. Equivalent blots were probed with unpurified anti-INR C-terminal serum (αINRct), anti-P2 (αp2), anti-phosphotyrosine (αpTyr), GST-p85/N-SH2 domain (p85/SH2) and GST/Grb2 (Grb2/SH2). Blots probed with αINRct, αp2 and αpTyr were developed by incubation with [^{125}I]protein A and autoradiography. Blots probed with GST fusion proteins were developed similarly with the exception that the incubation with [^{125}I]protein A was preceded by an incubation with a polyclonal anti-GST antiserum. Immunoreactive bands are shown by arrow heads and brackets indicate the IgG present in the immunocomplexes, seen in some of the blots. (**C**) Schematic representation of the two processing pathways of the INR precursor. The INR preproreceptor (Figure 2A) differential processing is illustrated by showing the two mature forms of INR generated, their disposition in the plasma membrane, and the differential phosphorylation state (-P) of the C-terminal extension (see text for details).

appeared to have an oligomeric structure similar to the mammalian insulin and IGF 1 receptors (Fernandez-Almonacid and Rosen, 1987). In addition, analysis of the topology of INR indicated that both β_{90} and β_{170} were disposed in a similar manner in the plasma membrane, suggesting that the additional sequence present in INR β_{170} mapped to the cytosolic face of the protein (Fernandez-Almonacid, 1992). Since we found no evidence indicating that a related gene or alternative splicing is responsible for INR protein diversity, we examined the possibility that the alternative forms are generated by processing a common preproreceptor encoded by the INR ORF. To test this, an *inr* minigene construct was subcloned in expression vectors that would enable overexpression of full-length or individual domains of INR in both *Drosophila* cell lines as well as in transgenic flies. Figure 3A shows a representative transient expression experiment in which an *inr* minigene (see Materials and methods), cloned under the control of the metallothionein promoter (pRmHa-INR), was either induced with $CuSO_4$ in serum-free medium, or induced with $CuSO_4$ followed by stimulation with insulin. Immunoblot analysis with antibodies raised against a peptide from the kinase region of the human insulin receptor that cross-reacts with INR (peptide P2, Fernandez-Almonacid and Rosen, 1987), recognized a single band of 170 kDa expressed only in the Cu^{2+}- induced S2/M3 cells, which appears to correspond to the unprocessed form of the INR β subunit (Figure 3A, αp2). The 170 kDa protein was also recognized by an antiserum raised against a GST fusion protein (GST-INR 1704) containing part of the C-terminal portion of INR (residues 1704–1997, data not shown), and by an affinity-purified fraction of this serum (Figure 3A, αINRct aff. pur.), obtained with a GST fusion protein extending from amino acid 1789 to 1997 (Figure 3C, GST-INR 1789). However, anti-INRct aff. pur. revealed an additional polypeptide of 60 kDa in total lysates of S2/S cells after transient transfections with pRmHa-INR (Figure 3A). Immunoblots with anti-P2 antiserum recognized the 170 kDa protein along with a 90 kDa β subunit type in these extracts (Figure 3A) whereas immunoblotting with the anti-INR C-terminal antiserum showed reactivity to all three subunits (170, 90 and 60 kDa) in both Triton X-100 lysates from transient S2/S transfectants (not shown), and in lysates from stable S2/S cell lines (Figure 3B, αINRct).

Immunoblot analysis with polyclonal anti-phosphotyrosine antibodies of total cell lysates from transient transfectants (not shown), or immunoprecipitated samples from stably transfected S2/S cells with anti-C-terminal antiserum (Figure 3B), show that both the 170 kDa and the 90 kDa, but not the 60 kDa protein are tyrosine phosphorylated upon insulin stimulation. To characterize further the nature of the tyrosine phosphorylation sites present in either the β_{90} or the β_{170} subunits, we have studied the interaction of these polypeptides with various SH2 domain-containing GST fusion proteins. These results indicate that the β_{170} subunit is specifically recognized by a fusion protein containing the SH2 domains of the p85 subunit of PI-3K (Figure 3B, p85/SH2), but not by the SH2 domain of Grb2 (Figure 3B, Grb2/SH2). The β_{90} was not recognized by either SH2 containing fusion protein, and the 60 kDa subunit does not react with any of the above-mentioned phosphotyrosine-specific probes. The reactivity of the β_{170} subunit is consistent with the deduced sequence that predicted the presence of YMXM motifs in the C-terminal tail of INR, and the absence of a consensus site (YL/VNE/D) for binding of the Grb2 SH2 domain in the C-terminal region of INR (Skolnik *et al.*, 1993). In addition, based on the reactivity of each polypeptide with various site-specific antibodies, anti-phosphotyrosine antibodies and GST SH2 fusion proteins, we propose (as shown schematically in Figure 3C) that the carboxy-terminal domain of the INR β_{170} subunit undergoes cell-specific proteolytic processing, resulting in the release of a free cytosolic, stable C-terminal fragment of 60 kDa and a concomitant appearance of the β_{90} subunit. This cleavage must occur downstream of the kinase domain, approximately between amino acids 1704 and 1789. Our results suggest that specific phosphorylation of the C-terminal extension of INR on YMXM motifs occurs only if this tail remains attached to the tyrosine kinase domain as is the case for the β_{170} subunit.

Since it has been shown that insulin treatment of *Drosophila* Schneider cells can stimulate the *Drosophila* MAP kinase homolog (Biggs and Zipursky, 1992), and since it has been demonstrated in mammalian cell systems that the HIR can phosphorylate Shc and activate the ras/MAPK cascade independent of IRS-1 (Myers *et al.*, 1994a,b), we propose that INR receptors lacking the C-terminal extension of the β_{170} subunit [$\alpha_2(\beta'_{90})_2$], could still retain the ability to activate the Ras/MAP kinase pathway, via tyrosine phosphorylation of a *Drosophila* Shc homolog (Ka-Man *et al.*, 1994). On the other hand, receptors containing the full-length β_{170} subunit [$\alpha_2(\beta_{170})_2$] should have an extended signaling potential that would allow them to simultaneously activate the Ras/MAP kinase, the PI-3 K and the p70S6 kinase signaling pathways; in a similar manner as demonstrated by L.Yenush *et al.* (in preparation) through expression of a chimeric human–*Drosophila* insulin receptor construct that carries the INR β_{170} subunit in the 32D myeloid progenitor cells.

The INR protein is abundantly expressed during embryogenesis and its function is required for normal development

Assuming that the high level of INR mRNA expression during embryogenesis (Petruzzelli *et al.*, 1986) is required for normal development, we decided to investigate whether loss of function in *inr* could result in recessive lethality. The *inr* gene was mapped by *in situ* hybridization to chromosomal region 93E1-3. Therefore, we tested candidate complementation groups mapping to the region uncovered by the deficiencies $Df(3R)e^{D7}$ and $Df(3R)e^{F1}$, which include 93E. Seven lethal complementation groups isolated in a screening for *tin*, *bap* and *S59* mutants (induced by EMS, see Azpiazu and Frasch, 1993), were mapped to the interval defined by the distal breakpoints of these two deficiencies, to which *inr* was mapped by Southern blot analysis (not shown). Thirty out of a total of 50 mutations (indicative of the large target size of the *inr* gene) which mapped in this genetic interval belonged to a complementation group identified as the *inr* gene. The identification of the *inr* complementation group was based on two criteria. First, a transgene that drives expression of the *inr* minigene under control of the heat shock promoter was able to rescue the lethality of several

Table I. Allelism between EMS-induced *inr* mutants and the PZ insertion 3-5545 and heat shock independent rescue by the *inr* transgene *hs-inr17, Df(3R)e^{D7}*

EMS allele	Allelism between *inr* mutants and 3-5545		HS-independent rescue by *hs-inr17,Df(3R)e^{D7}*
31	342/0[a]	–	180/10[c] (6%)
35	396/96[b]	24.2%	168/18 (11%)
74	270/0	–	108/20 (19%)
76	304/0	–	168/56 (33%)
87	338/110	32.5%	120/44 (36%)
117	272/84	30.8%	108/6 (6%)
167	234/0	–	124/26 (21%)
211	216/20	9.3%	124/50 (40%)
262	258/0	–	128/42 (33%)
277	234/72	30.8%	176/6 (3%)
301	358/0	–	136/32 (18%)
306	336/104	31%	110/12 (11%)
310	194/0	–	140/24 (17%)
327	200/0	–	136/50 (36%)
353	296/0	–	114/24 (21%)
PZ3-5545	N/A	N/A	192/34 (18%)

[a]Stocks used were *PZ 3-5545/MKRS* and *inr^{EMS}/TM3Sb*. Numbers x/y represent the total numbers of flies scored (x), and (y) corresponds to the number of non-Stubble flies. When applicable, the percentage of viability of a given heteroalleleic combination is shown. With fully viable combinations, 33% of non-Stubble flies are expected.
[b]All viable heteroallelic combinations showed a minute-like phenotype.
[c]x/y represent the total numbers of flies scored (x), and the number of flies of the genotype *inr^{x}/hs-inr17,Df(3R)eD7* (y), respectively. The fraction of (y) over (x), as percentage, is shown in parentheses. (Full rescue would theoretically yield 33% of these flies.)
N/A, not applicable.

alleles *in trans* to the *Df(3R)e^{D7}* of this, but not other, complementation groups (Table I). Second, a lethal mutation caused by a P-element insertion in 93E was allelic to this group as well (Table I). We determined the insertion site of this P-element (PZ3-5545, Karpen and Spradling, 1992) molecularly, and found it to be inserted into the *inr* coding region close to the 5′ end (Figure 1). The results presented in Table I show that the PZ 3-5545 (*inr^{PZ}*) insertion is not viable over most of the EMS induced *inr* alleles; however, six heteroallelic combinations show different degrees of viability. Similarly, a complex pattern of interallelic complementation was observed among the EMS alleles themselves (see Table II). We have not found a single allele that behaves like the deficiencies used to screen for lethals in this region and fails to complement all other members of this group, suggesting that all of our mutants are hypomorphs. The occasional ability of different *inr* alleles to complement one another is consistent with the dimeric nature of the receptor and also with an intermolecular molecular mechanism for autophosphorylation that has been previously established for receptor tyrosine kinases (Lemmon and Schlessinger, 1994). Similar observations of heteroallelic complementation with hypomorphic alleles were previously made with mutations in the *Drosophila* EGF receptor homolog, whose activity is also dependent upon receptor dimerization (Raz *et al.*, 1991; Clifford and Schupbach, 1994).

To establish the nature of the embryonic lethality associated with loss of function of *inr*, we first studied the expression pattern of INR protein during embryogenesis. Figure 4 shows whole mount embryo immunostainings

Table II. Interallelic complementation

inr allele No.	**35**	**217**	**219**	**273**	**304**	**313**	**327**
35		275/0	300/0	204/22[a]	268/38	418/114	237/67
217			474/0	260/0	237/0	214/0	178/0
219				279/0	248/0	290/0	378/0
273					264/0	536/158	132/0
304						396/0	566/0
313							382/24

[a]*inr* mutants were generated on *rutipa* chromosomes (see Materials and methods); either *rutipa/TM3Sb* or *rutipa/TM1Me* stocks were used in these crosses. Numbers (x/y) correspond to the total number of flies scored (x) and (y) represents the heteroallelic survivors scored as *rutipa* homozygous. Full viability would yield 25% as transheterozygous. Most viable heteroallelic combinations showed also a minute-like phenotype.

obtained with an anti-INR C-terminal antiserum. As expected, the INR protein is both abundantly and widely distributed from the initiation of cellularization to the onset of gastrulation (Figure 4A and B). This is consistent with the previously reported presence of homogeneously distributed, maternally inherited INR transcripts in unfertilized eggs (Petruzzelli *et al.*, 1986; Garofalo and Rosen, 1988). By stages 9–11 of embryogenesis, INR expression is evident in all three germ layers of fully germ band-extended embryos. The posterior midgut primordium, epidermis and neuroblasts show high levels of INR protein, whereas the mesoderm is only lightly stained (Figure 4B). By stage 12, when zygotic INR transcripts have accumulated to a maximum, INR protein is highly expressed throughout the epidermis, in the migrating midgut primordia, hindgut and a segmental pattern of staining in the developing ventral cord becomes more evident (Figure 4C and D). Although the epidermal and gut expression of INR decays as development proceeds, by stage 16, the staining of the ventral cord persists and includes both the cellular bodies and the axon tracts (Figure 4E and F). By stage 17, only the ventral cord and supraesophageal ganglion of the developing brain remain immunoreactive (Figure 4G). Since INR expression is so ubiquitous during most stages of embryogenesis, we performed antibody staining on embryo collections derived from *Df(3R)e^{D7}*/TM3 flies to establish the specificity of the anti-INR antiserum. A stage 16 homozygous deficiency embryo (identified by its *tin/bap* phenotypes, Azpiazu and Frasch, 1993), shows virtually no immunoreactivity, when compared with a heterozygous deficiency embryo (Figure 4H and F, respectively). In contrast, stage 16 embryos that are homozygous for a *Df(3R)e^{D7}* chromosome which carries a heat shock-inducible minigene, *HS-inr17*, display ubiquitous and high levels of INR protein expression, even in the absence of heat shock induction (Figure 4J). The ability of this transgenic line to produce high basal levels of INR protein is in agreement with the successful rescue of all *inr* alleles tested in the absence of heat shock (Table I). As shown in Figure 4I, the PZ-insertion 3-5545 causes a severe reduction in the level of INR expression in *inr^{PZ}* homozygous embryos. Although these embryos appear to be largely depleted of INR protein, expression localized to the hindgut, posterior spiracles and the staining at the most anterior epidermal tip appears to be at normal levels. Considering the facts that: (i) the PZ insertion

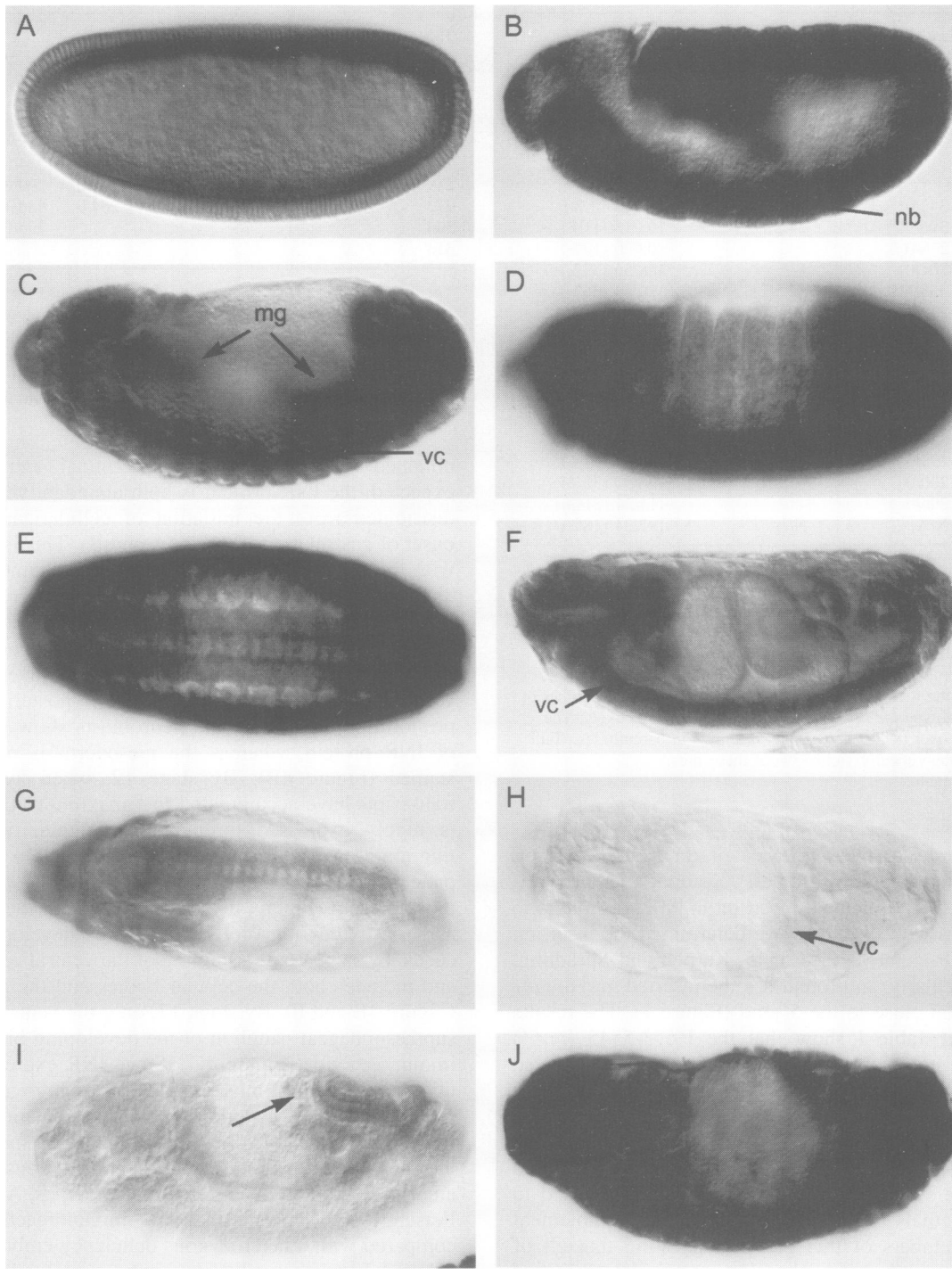

Fig. 4. Immunolocalization of the INR protein during embryogenesis using anti-INR C-terminal polyclonal antiserum. Embryonic expression of INR protein was assessed by whole mount immunostaining of embryos collected from *Df(3R)e^{D7}/TM3* flies. Staining was carried out with αINRct antiserum (see Materials and methods). A representative homozygous *Df(3R)e^{D7}* (ventro–lateral view, stage 16, all staging is according to Campos-Ortega and Hartenstein, 1985) is shown in (**H**). Lateral (**A–D** and **F**), and ventral (**E** and **G**) views of deficiency heterozygous embryos show INR expression in a cellularized blastoderm (**A**), and in germ band extended embryos (**B**, stage 11), indicating the staining of the posterior midgut primordium (pm), neuroblasts (nb) and ventral epidermis (out of focus). Different views of embryos at stages 10–12, focused on the midgut (mg) primordia and the developing ventral cord (vc); lateral (**C**), or ventral (**E**) views. Panel (**D**) shows the same embryo as in (C), focused on the epidermis. The nerve cord reactivity is also shown in an older embryos, stage 17 (panel **G**). A lateral view (**I**) of a PZ 3-5545 homozygous embryo stained with anti-INR, is shown to illustrate the residual expression of the receptor observed in stage 12 embryo. Anti-INR immunostaining of homozygous embryos of the genotype *Df(3R)e^{D7}, HS-inr17* (**J**) shows the high basal levels of receptor expression of this transgenic line. All embryos were oriented anterior to the left, and photographed under Nomarski optics.

occurs in the first coding exon of the ORF reported here, whose only function may be to provide a signal peptide for membrane insertion of INR; (ii) the PZ insertion deletes most, but not all, of the INR embryonic protein expression; and (iii) some EMS alleles are viable over the *inr^{PZ}* allele. We propose that the PZ insertion knocks out

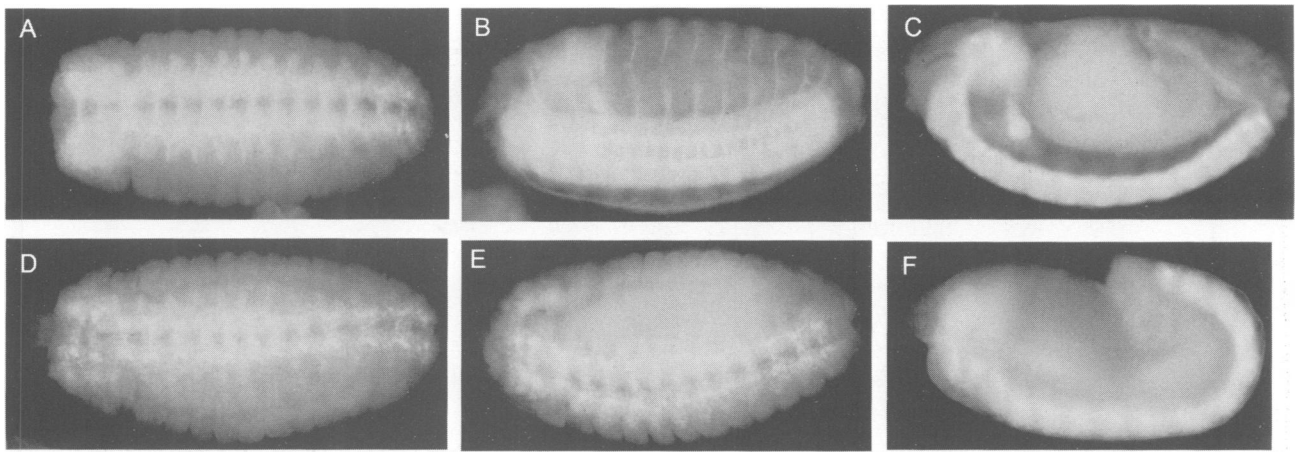

Fig. 5. *inr* is required for the development of the central nervous system. Nerve cord development was analyzed by whole mount embryo immunostaining with fluorescein-conjugated anti-HRP antibodies which specifically stain axon bundles and neuronal bodies of the ventral cord scaffold. (**A**) and (**D**) show ventral views of stage 12 embryos, whereas (**B**) and (**E**) show ventro–lateral views of stage 14–15 embryos. (A) and (B) are wild-type and (D) and (E) are inr^{PZ}/inr^{PZ} mutants. (**C**) and (**F**) correspond to lateral views of stage 14–15 wild-type (E) and inr^{353}/inr^{353} (F) mutant embryos. All embryos were oriented anterior to the left.

the gene product derived from the major (11 kb) embryonic INR transcript (Petruzzelli *et al.*, 1986). The INR activity remaining in PZ 3-5545 homozygous might be due to products generated by alternative splicing (i.e. the minor 8.5 kb INR transcript, Petruzzelli *et al.*, 1986) that could bypass the P-element insertion by using an exon located further upstream that encodes a different signal peptide.

Loss of function in inr induces pleiotropic phenotypes in the development of the embryonic nervous system

Because the maternally inherited INR transcripts (Petruzzelli *et al.*, 1986; Garofalo and Rosen, 1988) appear to be able to rescue, and therefore mask, early embryonic phenotypes (see below), we concentrated our attention on analysing the role of *inr* in the late development of the epidermis and the central nervous system. First we probed homozygous inr^{PZ} embryos, since these appear to lack all INR immunoreactivity in the ventral cord, or EMS alleles that produced non-viable heteroallelic combinations with inr^{PZ} (i.e. inr^{76}, inr^{301}, inr^{353}) with anti-HRP antiserum, which stains all neuronal cells and the axonal scaffolding of the CNS as well as sensory neurons and peripheral nerves in the PNS (Jan and Jan, 1982). A comparison of the central nervous system development in wild-type and *inr* mutant embryos, as revealed by fluorescein-labeled anti-HRP immunohistochemistry, is shown in Figure 5. This analysis indicates that by stage 12 of embryogenesis (Figure 5A and D) or later in development (stages 14–15, Figure 5B and E), inr^{PZ} homozygotes display a severe decrease in the total immunoreactivity of neuronal bodies. Defects are also obvious in the process of condensation of the neuropile, since neither longitudinal connectives nor the commissures form normally. The longitudinal tracts are poorly condensed and often interrupted, and the anterior and posterior commissures are apparently fused and not condensed. In addition, the nerves that form the anterior fascicles (compare Figure 5B and E) and the developing brain (compare Figure 5C and F) also show a significant decrease in their typical HRP immunoreactivity. The CNS phenotype observed in inr^{PZ} homozygotes was consistently seen in homozygotes of several EMS alleles, as with these alleles *in trans* to the PZ insertion or $Df(3R)e^{D7}$. Strikingly, inr^{353}/inr^{353} mutants (Figure 5F), and similarly four other alleles (inr^{35}, inr^{232}, inr^{242} and inr^{327}) displayed additional defects at earlier stages of development. These mutants showed a failure in the process of germ band retraction, both as homozygotes or in trans to $Df(3R)e^{D7}$. This phenotype was not typically seen in inr^{PZ} or deficiency homozygous, and it was only slightly reduced in some cases when analyzed *in trans* to $Df(3R)e^{D7}$. A possible explanation for this could be that the zygotic and maternal gene products can interact (i.e. heterodimerize), and therefore, a zygotically produced mutant protein could block the activity of the maternally inherited wild-type INR by acting in a dominant negative manner. Notably, such a mechanism has been recently proposed to account for similar genetic interactions between mutations in gene products that are also expressed in the early embryo from both maternal and zygotic mRNAs (Doyle and Bishop, 1993; Littleton and Bellen, 1994). Analysis of cuticles derived from these mutants indicate that in addition to the lack of germ band retraction, dorsal closure does not occur, there is an occasional decrease in the width of denticle belts, and severe defects in head structures are also observed (Figure 7), similar to *faint little ball* embryos that correspond to mutations in the *Drosophila* EGF receptor (Raz and Shilo, 1992; Clifford and Schupbach, 1992). In contrast, the cuticle patterns in mutants for the other alleles that were examined appear to be normal. Although the generation of germ line chimera will ultimately prove the role of the maternal contribution of *inr* in early development, our data suggests that *inr* may play some role in the establishment or maintenance of dorso-ventral polarity.

To extend our analysis of the nervous system development in *inr* mutants, we also performed immunostaining with mAb 22C10 (Fujita *et al.*, 1982). This antibody labels all neurons of the peripheral nervous system, and also a limited number of neurons in the nerve cord. As shown in Figure 6B and E, inr^{PZ}/inr^{301} embryos show virtually no mAb 22C10 immunoreactivity in the ventral cord, with the exception of a single cell indicated in the midline, and one or two immunoreactive neurons in the longitudinal

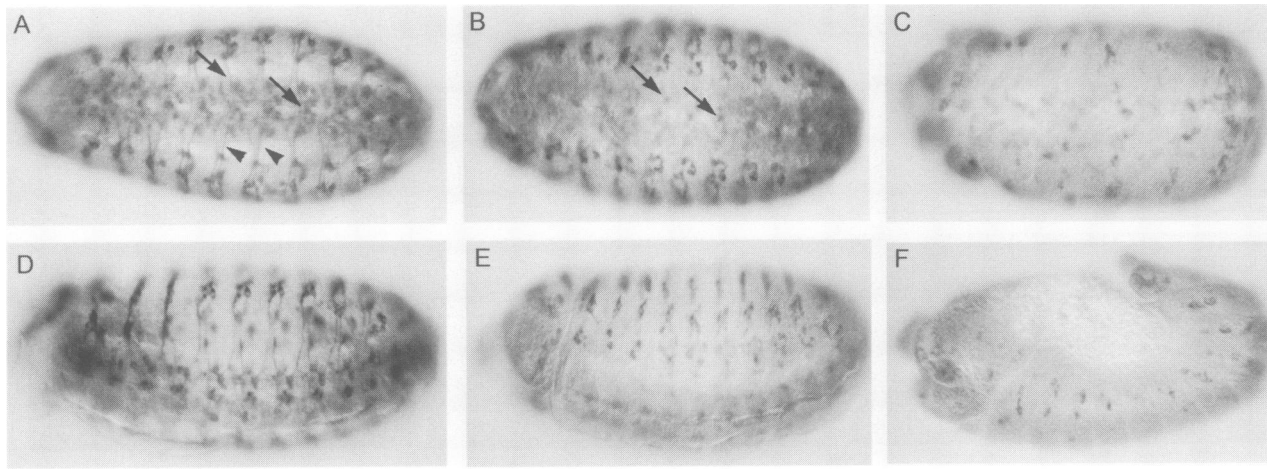

Fig. 6. Development of the peripheral and central nervous system in *inr* mutants probed with mAb 22C10. Organization of the ventral cord and PNS, as revealed by immunohistochemistry with mAb 22C10 is shown in ventral views (stage 15; **A** and **B**) or ventro–lateral views (stage 12; **D** and **E**) of wild-type (A and D) and inr^{PZ}/inr^{301} (B and E) mutant embryos. Panels **C** and **F** show ventral and lateral views, respectively, of inr^{353}/inr^{353} homozygous embryos. Arrows point to 22C10 immunoreactive neurons of the ventral cord that develop normally in *inr* mutants, whereas arrowheads point to the anterior and posterior fascicles, which along with most of the remaining mAb 22C10 immunoreactivity of the nerve cord and the most ventral sensory neurons, are missing in inr^{PZ}/inr^{301} embryos. All embryos were oriented anterior to the left, and photographed under Nomarski optics.

tracts, as compared with a four- to five-cell cluster in wild-type embryos (Figure 6A and B). In addition, as shown in Figure 6D and E, there is a decrease in the 22C10 immunoreactivity in the PNS. The ventral-most sensory organs and the anterior and posterior fascicles do not appear to develop; fewer neurons are also detected in more dorsal sensory organs. Homozygous inr^{353} mutants (Figure 6C and F) show a more severe phenotype with respect to the development of the PNS , which could be due to depletion of maternally supplied wild-type products, as discussed above. Since the reduced immunoreactivity of neuronal markers observed in *inr* mutants is manifested by stages 11–12 of embryogenesis, we determined whether the development of earlier neuroblasts markers, as well as other neuronal cell types such as glia, are also affected in *inr* mutants. Immunostaining with anti-RK2 antiserum, which recognizes a glial-specific homeodomain protein that is expressed throughout glial development and in most embryonic glia (Campbell,G. *et al.*, 1994), as well as immunostaining with antibodies that recognize segment polarity gene products expressed in different neuroblast populations (Chu-LaGraff and Doe, 1993) suggests that the development of multiple neuroblast lineages are affected in *inr* mutants (data not shown). These observations are consistent with recent findings indicating that, in *Drosophila*, several neuronal lineages give rise to both neurons and glia (Udolph *et al.*, 1993; Bossing and Technau, 1994; Condron and Zinn, 1994). Although a more detailed analysis of these phenotypes is required, our data suggests that *inr* plays a key role during neurogenesis, since large populations of both neurons and glia do not develop in *inr* mutant embryos. This might be indicative of a failure of some multipotent neuroblast precursors to proliferate. However, we cannot rule out the possibility that *inr* may play a supporting or trophic role in developing multipotent neuronal precursors. Alternatively, *inr* may function to induce neuronal cell fate determination, as is the case for other RTKs such as *sevenless* (Zipursky and Rubin, 1994) and the *Drosophila* EGF receptor (Freeman, 1994; Tio *et al.*, 1994) in the specification of photoreceptors during development of the eye imaginal disc.

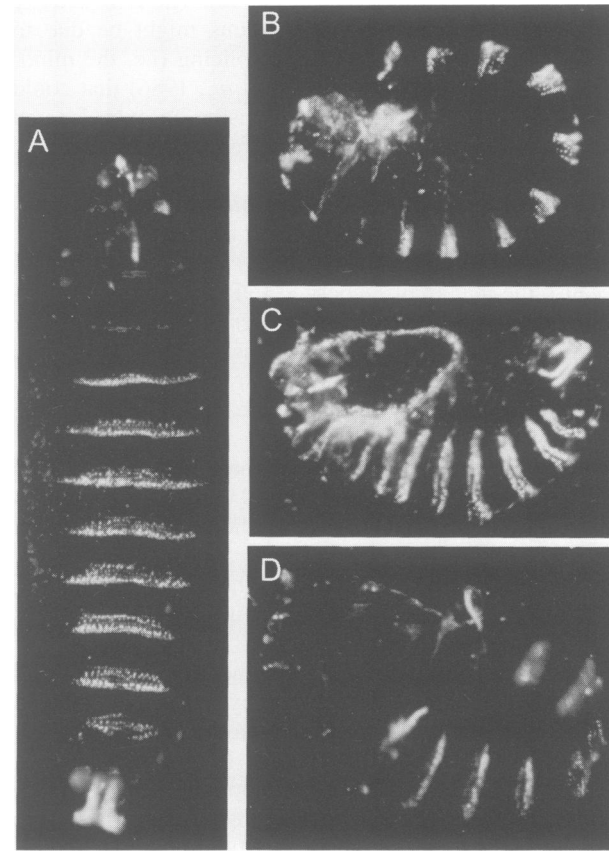

Fig. 7. Cuticle phenotypes of embryonic lethal *inr* mutants that show dominant negative effects. Pleiotropic phenotypes affecting cuticle development were observed in embryos homozygous for various *inr* alleles (inr^{35}, inr^{232}, inr^{242}, inr^{327} and inr^{353}). These phenotypes were characterized by tight curling of the cuticles reflecting lack of germ band retraction (**B**), as compared with those derived from wild-type larvae (**A**). Also shown are cuticles with incomplete dorsal closure (**C**), narrower (in the dorso-ventral direction) denticle bands (**D**) and missing head structures (B, C and D). Cuticles shown in (B) and (D) correspond to inr^{353} homozygotes, whereas (C) corresponds to an $inr^{353}/Df(3R)e^{D7}$ embryo. Photographs were taken under dark field.

Concluding remarks

We have described the cloning of the *inr* gene, which encodes the *Drosophila melanogaster* homolog of the mammalian insulin receptor. One major conclusion that can be drawn from our molecular genetic analysis of *inr* is that the predicted structural complexity of *Drosophila* insulin receptors, as originally determined from biochemical studies, can be attributed to the differential proteolytic processing of a single INR proreceptor molecule. Another important result is that INR appears to play a critical role during neurogenesis, as revealed by the mutational analysis of the *inr* locus. This phenotype is reminiscent of some of the defects in proliferation of neuroblasts associated with the targeted disruption of the mouse genes for the IGF 1 receptors and its ligands IGF 1, and IGF 2. It is possible that, similar to the *Drosophila* EGF receptor (which is a unique homolog of all four mammalian EGF/neu/heregulin receptor genes, *erb1–erb4*), a single *Drosophila* insulin receptor gene may fulfil all functions attributed to the family of mammalian insulin and IGF 1 receptors. Accordingly, *inr* mutations could also manifest themselves later in *Drosophila* larval development, leading to alterations in cellular metabolism.

Materials and methods

Antibodies

The anti-peptide antibody to the kinase domain of HIR that cross-reacts with INR (anti-P2) has been previously described (Fernandez-Almonacid and Rosen, 1987). Polyclonal antisera against a GST fusion protein that contains part of the C-terminal extension of INR (from residues 1704–1997) were raised in rabbits by injecting affinity-purified GST fusion protein. This and all other GST fusion proteins were prepared by affinity chromatography on glutathione agarose columns according to Smith and Johnson (1988). Rabbit polyclonal antisera to phosphotyrosine and to purified GST were described by Batzer *et al.* (1994). Antibodies to the homeodomain protein RK-2 (G.Campbell *et al.*, 1994) and mAb 22C10 (Fujita *et al.*, 1982) were generously provided by Drs A.Tomlinson and S.Benzer, respectively. Fluorescein-conjugated anti-HRP antibodies were purchased from Cappel. A monoclonal anti-β galactosidase antibody used to identify embryos that did not carry a *TM3Sb,ftzlacZ* balancer (homozygous mutants) or that were inr^{PZ} homozygous was purchased from Promega.

Cell lines, transfections, immunoprecipitations and immunoblotting

The *Drosophila* Schneider cell line 2 (referred to as S2/S), and a clone derived from this line (referred to as S2/M3) were grown in Schneider and M3 medium, respectively, supplemented with 12% fetal bovine serum, 100 U/ml penicillin and 100 μg/ml streptomycin. Both of these cells lines were obtained from Dr L.Cherbas, and cultures were maintained at room temperature. For transfection assays, the *inr* minigene construct (see below) was cloned into the *Eco*RI site of the pRmHa3 expression vector (Bunch *et al.*, 1988). This construct is referred to as pRmHa-INR. Transient transfections, using the *N,N*-bis(2-hydroxyethyl)-2 aminoethane sulfonic acid (Bes)/calcium phosphate co-precipitate method, were carried out as described by Bunch and Brower (1992). To isolate stably transfected pools expressing INR, cells were co-transfected with pRmHa-INR and pPC4 (Jokerst *et al.*, 1989) plasmids and selected with 5–10 μg/ml of α-amanitin (Sigma).

For induction of INR expression, overexpressing cells were incubated in either Schneider or M3 medium containing 0.1% calf serum and 0.7 mM $CuSO_4$ for 30 h. After induction, cells were washed three times in PBS, resuspended in M3 medium containing 0.1% calf serum and left untreated (quiescent) or stimulated with insulin (recombinant porcine insulin was a generous gift from Eli Lilly Co.). After insulin treatment, cells were immediately placed on ice, washed twice in ice-cold PBS and lysed in 50 mM *N*-2-hydroxyethyl-1-piperazine-*N*'-2-ethanesulfonic acid (HEPES), 10% glycerol, 150 mM NaCl, 2 mM EDTA, 2 mM EGTA, 25 mM NaF, 1 mM sodium orthovanadate and 10 μg/ml of leupeptin, aprotinin and pepstatin. Total cell lysates or immunoprecipitates were analyzed by SDS–PAGE and immunoblotting after electrotransfer to nitrocellulose, as described by Margolis *et al.* (1989).

cDNA and genomic cloning

cDNAs were isolated from an 8–12 h embryonic λgt10 cDNA library (Poole *et al.*, 1985). Genomic clones were isolated from a CaSpeR cosmid library (obtained from Dr J.Tamkun) and from a λEMBL4 library (not shown in Figure 1), provided by M.Noll (University of Zurich). Nested deletions with exonuclease III (Erase-a-Base kit, Promega) were generated to sequence cDNA clones. Sequence gaps were filled with custom-made oligonucleotide primers. Genomic subclones were also sequenced with specific primers. Sequencing was carried out on double-stranded plasmid DNA with Sequenase (USB). Sequencing, Northern and Southern blotting, plaque and colony screening, PCR, 5'RACE, RT–PCR and other cloning techniques were performed according to Berger and Kimmel (1987) or Sambrook *et al.* (1989).

The minigene construct that enabled us to express the full-length INR protein was generated as follows: a 7.6 kb *Eco*RI–*Afl*II genomic fragment covering the 5' end portion of the ORF, from upstream of the methionine start site assigned in Figure 1 to the middle of the kinase domain (nucleotide position 4414 in the sequence shown on Figure 1), was ligated to a 2.8 kb *Afl*II–*Eco*RI cDNA fragment obtained from clone βA3.1. These fragments were ligated into the *Eco*RI site of the Bluescript vector (Stratagene). Genomic sequences preceding the translational start site of the ORF were deleted by replacing a 1.5 kb *Sal*I–*Eco*47III fragment, extending from the polylinker to nucleotide 978 in the sequence shown in Figure 1, with a 802 bp PCR fragment covering from nucleotides 176 to 978. This PCR product was synthesized from cosmid S8 using the oligonucleotide primers: 5'-GCGGTCGACGAATTCAA-CTCAAGAAATGTTGCTGGATACATG-3' (forward) and 5'-GCGGT-CGACTTCGAATTCGCTCCTTGGCCATCGCGTTTGCG-3' (reverse). The forward primer contained an *Eco*RI site (underlined) to allow us to excise the *inr*-minigene as a 9.5 kb *Eco*RI fragment, which was subsequently subcloned into the *Eco*RI site of the expression vectors pRmHa3 or pCasper-hs, for *Drosophila* cell line transfections or germ line transformation of flies and rescue of *inr* mutants, respectively.

Antibody staining and cuticle preparations

Whole mount immunostaining of embryos was performed as described by Ashburner (1989). Anti-INR C-terminal antiserum was diluted 1:10 000. Primary antibodies were detected with the ABC-elite kit (Vector Laboratories). Staining with fluorescein-conjugated anti-HRP antiserum was also performed in whole mounts. After antibody incubations and washes, embryos were post-fixed in PBS containing 2% paraformaldehyde and mounted in Citifluor (UKC Chemical Laboratory). Cuticles were prepared essentially as described by Wieschaus and Nusslein-Volhard (1986), with the modifications recommended by Cadigan *et al.* (1994). Embryos were photographed under fluorescence, Nomarski or dark field using a Zeiss Axiophot microscope and Ektachrome 160T or TMAX100 films. Slides or prints were processed with Adobe Photoshop for Macintosh (version 2.5.1).

Genetic protocols

The screening for recessive lethals in the region uncovered by the deficiencies $Df(3R)e^{D7}$ and $Df(3R)e^{F1}$ was described by Azpiazu and Frasch (1993). The cytological characterization of the PZ element (Karpen and Spradling, 1992) insertion, PZ3-5545, was carried out in the Rubin laboratory, and the line was kindly provided to us by T.Laverty. The genomic sequences flanking this P-element were isolated by plasmid rescue (Azpiazu and Frasch, 1993), and the insertion site was determined by sequencing with a primer that hybridizes with the P-element inverted repeat sequences. For P-element-mediated rescue of *inr* mutants, the *inr* minigene was subcloned into the *Eco*RI site of the transformation vector pCasper-hs (Ashburner, 1989). An insertion on the third chromosome (*HS-inr17*) was first recombined onto the deficiency chromosome $Df(3R)e^{D7}$, and then used *in trans* to the mutagenized chromosomes to test its rescue activity. An independent insertion in the second chromosome (*HS-inr7*) was also obtained and successfully used in rescue experiments. Rescue activity was assessed by scoring for survival of non-Stubble flies when using *TM3Sb* or *MKRS* balanced stocks.

Accession number

The accession number for the sequence reported in this paper is U28136.

Acknowledgements

This manuscript is dedicated *in memoriam* to Dr Ora M.Rosen in whose laboratory this work was initiated. R.F. and D.T. wish to thank Drs Ken

Marians and Jerry Hurwitz for their continuous support of this work. We also thank Cord Dohrmann and Renee Garcia-Arenas for isolating genomic cosmid and phage clones. N.A. was supported by a fellowship from the Basque country and M.F. by a grant from the NIH (HD 30832) and by a scholarship from the Pew foundation.

References

Andersen,A.S., Kjeldesen,T., Wiberg,F.C., Vissing,H., Schaffer,L., Rasmussen,J.S., De Meyts,P. and Moller,N.P.H. (1992) *J. Biol. Chem.*, **267**, 13681–13686.

Ashburner,M. (1989) *Drosophila: A Laboratory Manual.* Cold Spring Harbor Laboratory Press, Cold Spring Harbor, NY.

Azpiazu,N. and Frasch,M. (1993) *Genes Dev.*, **7**, 1325–1340.

Backer,J.M., Shoelson,S.E., Weiss,M.A., Hua,Q.X., Cheatham,R.B., Haring,E., Cahill,D.C. and White,M.F. (1992) *J. Cell Biol.*, **118**, 831–839.

Batzer,A.G., Rotin,D., Urena,J.M., Skolnik,E.Y. and Schlessinger,J. (1994) *Mol. Cell. Biol.*, **14**, 5192–5201.

Benito,M., Porras,A., Nebreda,A.R. and Santos,E. (1991) *Science*, **253**, 565–568.

Berger,S.L. and Kimmel,A.R. (eds) (1987) *Methods Enzymol.*, **152**.

Biggs,W.H.,III and Zipursky,S.L. (1992) *Proc. Natl Acad. Sci. USA*, **89**, 6295–6299.

Bork,P. and Margolis,B. (1995) *Cell*, **80**, 693–694.

Bossing,T. and Technau,G.M. (1994) *Development*, **120**, 1895–1906.

Bowtell,D.D.L., Simon,M.A. and Rubin,G.M. (1988) *Genes Dev.*, **2**, 620–634.

Bunch,T.A. and Brower,D.L. (1992) *Development*, **116**, 239–247.

Bunch,T.A., Grinblat,Y. and Goldstein,L.S.B. (1988) *Nucleic Acids Res.*, **16**, 1043–1061.

Cadigan,K.M., Grossniklaus,U. and Gehring,W.J. (1994) *Genes Dev.*, **8**, 899–913.

Campbell,G., Goring,H., Lin,T., Spana,E., Andersson,S., Doe,C.Q. and Tomlinson,A. (1994) *Development*, **120**, 2957–2966.

Campbell,K.S., Ogris,E., Burke,B., Su,W., Auger,K.R., Druker,B.J., Schaffhausen,B.S., Roberts,T.M. and Pallas,D.C. (1994) *Proc. Natl Acad. Sci. USA*, **91**, 6344–6348.

Campos-Ortega,J.A. and Hartenstein,V. (1985) *The Embryonic Development of Drosophila melanogaster.* Springer-Verlag, Berlin.

Cavener,D.R. and Ray,S.C. (1991) *Nucleic Acids Res.*, **19**, 3185–3192.

Cheatham,B., Vlahos,C.J., Cheatham,L., Wang,L., Blenis,J. and Kahn,C.R. (1994) *Mol. Cell. Biol.*, **14**, 4902–4911.

Chu-LaGraff,Q. and Doe,C.Q. (1993) *Science*, **261**, 1584–1597.

Chung,J., Grammer,T.C., Lemon,K.P., Kazlauskas,A. and Blenis,J. (1994) *Nature*, **370**, 71–75.

Clifford,R. and Schupbach,T. (1992) *Development*, **115**, 853–872.

Clifford,R. and Schupbach,T. (1994) *Genetics*, **137**, 531–550.

Condron,B.G. and Zinn,K. (1994) *J. Neurosci.*, **14**, 5766–5777.

De Meyts,P. (1994) *Diabetologia*, **37**, S135–S148.

Dohrmann,C., Azpiazu,N. and Frasch,M. (1990) *Genes Dev.*, **4**, 2098–2111.

Doyle,H.J. and Bishop,J.M. (1993) *Genes Dev.*, **7**, 633–646.

Ebina,Y. *et al.* (1985) *Cell*, **40**, 747–758.

Fabry,M., Schafer,E., Ellis,L., Korjo,E., Fahrenholz,F. and Brandenburg,D. (1992) *J. Biol. Chem.*, **267**, 8950–8956.

Fernandez-Almonacid,R. (1992) *The Drosophila melanogaster Insulin Receptor Homolog: Biochemical Characterization and Molecular Cloning.* PhD thesis, Cornell University.

Fernandez-Almonacid,R. and Rosen,O.M. (1987) *Mol. Cell. Biol.*, **7**, 2718–2727.

Fingar,D.C. and Birnbaum,M.J. (1994) *J. Biol. Chem.*, **269**, 10127–10132.

Fingar,D.C., Hausdorff,S.F., Blenis,J. and Birnbaum,M.J. (1993) *J. Biol. Chem.*, **268**, 3005–3008.

Freeman,M. (1994) *Mech. Dev.*, **48**, 25–33.

Fujita,S.C., Zipursky,S.L., Benzer,S., Ferrrus,A. and Shotwell,S.L. (1982) *Proc. Natl Acad. Sci. USA*, **79**, 7929–7933.

Garofalo,R.S. and Rosen,O.M. (1988) *Mol. Cell. Biol.*, **8**, 1638–1647.

Hausdorff,S.F., Frangioni,J.V. and Birnbaum,M.J. (1994) *J. Biol. Chem.*, **269**, 21391–21394.

Jan,L.Y. and Jan,Y.N. (1982) *Proc. Natl Acad. Sci. USA*, **79**, 2700–2704.

Jokerst,R.S., Weeks,J.R., Zehring,W.A. and Grennlaf,A.L. (1989) *Mol. Gen. Genet.*, **215**, 266–275.

Ka-Man,V.L., Olivier,J.P., O'Bryan,J., Henkemeyer,M., Pellici,P.G. and Pawson,T. (1994) Abstract. Tenth Annual Meeting on Oncogenes, Frederick, MD.

Kahn,C.R. (1994) *Diabetes*, **43**, 1066–1084.

Kappeller,R. and Cantley,L.C. (1994) *BioEssays*, **16**, 565–576.

Karpen,G.H. and Spradling,A.C. (1992) *Genetics*, **132**, 737–753.

Keller,S.R. and Lienhard,G.E. (1994) *Trends Cell Biol.*, **4**, 115–119.

Lee,J.J., von Kessler,D.P., Parks,S. and Beachy,P.A. (1992) *Cell*, **71**, 33–50.

Lemmon,M.A. and Schlessinger,J. (1994) *Trends Biochem. Sci.*, **19**, 459–463.

Lindsley,D.L. and Zimm,G.G. (1992) *The Genome of Drosophila melanogaster.* Academic Press, San Diego, CA.

Littleton,J.T. and Bellen,H.J. (1994) *Genetics*, **138**, 111–123.

Margolis,B.S., Rhee,S.G., Felder,S., Mervic,M., Lyall,R., Levitzki,A., Ullrich,A., Zillberstein,A. and Schlessinger,J. (1989) *Cell*, **57**, 1101–1107.

Ming,X.-F., Burgering,B.M.Th., Wennstrom,S., Claesson-Welsh,L., Heldin,C.H., Bos,J.L., Kozma,S.C. and Thomas,G. (1994) *Nature*, **371**, 426–429.

Mount,S.M., Burks,C., Hertz,G.D., Stormo,G., White,O. and Fields,C. (1992) *Nucleic Acids Res.*, **20**, 4255–4262.

Myers,M.G.,Jr, Sun,X.J. and White,M.F. (1994a) *Trends Biochem. Sci.*, **19**, 289–293.

Myers,M.G.,Jr, Grammer,T.C., Wang,L.-M., Sun,X.J., Pierce,J.H., Blenis,J. and White,M.F. (1994b) *J. Biol. Chem.*, **269**, 28783–28789.

Nishida,Y., Hata,M., Nishizuka,Y., Rutter,W.J. and Ebina,Y. (1986) *Biochem. Biophys. Res. Commun.*, **141**, 474–481.

O'Neill,T.J., Craparo,A. and Gustafson,T.A. (1994) *Mol. Cell. Biol.*, **14**, 6433–6442.

Pawson,T. and Schlessinger,J. (1993) *Curr. Biol.*, **3**, 434–442.

Petruzzelli,L., Herrera,R. Garcia,R. and Rosen,O.M. (1985) *Cancer Cells.* Cold Spring Harbor Laboratory Press, Cold Spring Harbor, NY, vol. 3, pp. 115–121.

Petruzzelli,L., Herrera,R., Arena-Garcia,R., Fernandez,R., Birnbaum,M.J. and Rosen,O.M. (1986) *Proc. Natl Acad. Sci. USA*, **83**, 4710–4714.

Poole,S.J., Kauvar,L.M., Drees,B. and Kornberg,T. (1985) *Cell*, **40**, 37–43.

Porras,A., Nebreda,A.R., Benito,M. and Santos,E. (1992) *J. Biol. Chem.*, **267**, 21124–21131.

Raz,E. and Shilo,B.Z. (1992) *Development*, **114**, 113–123.

Raz,E., Schejter,E.D. and Shilo,B.Z. (1991) *Genetics*, **129**, 191–201.

Robinson,L.J., Razzck,Z.F., Lawrence,J.C.,Jr and James,D.E. (1993) *J. Biol. Chem.*, **268**, 26422–26427.

Sambrook,J., Fritsch,E. and Maniatis,T. (1989) *Molecular Cloning: A Laboratory Manual.* 2nd edn. Cold Spring Harbor Laboratory Press, Cold Spring Harbor, NY.

Schäffer,L. (1994) *Eur. J. Biochem.*, **221**, 1127–1132.

Schumacher,R., Mosthaf,L., Schlessinger,J., Branderburg,D. and Ullrich,A. (1991) *J. Biol. Chem.*, **266**, 19288–19295.

Skolnik,E.Y. *et al.* (1993) *EMBO J.*, **12**, 1929–1936.

Smith,D.B. and Johnson,K.S. (1988) *Gene*, **67**, 31–40

Sun,X.L., Rothenberg,P., Kahn,C.R., Backer,J.M., Araki,E., Wilden,P.A., Cahill,D.A., Golstein,B.J. and White,M.F. (1991) *Nature*, **352**, 73–77.

Tio,M., Ma,C. and Moses,K. (1994) *Mech. Dev.*, **48**, 13–23.

Udolph,G., Prokop,A., Bossing,T. and Technau,G.M. (1993) *Development*, **118**, 765–775.

Ullrich,A. *et al.* (1985) *Nature*, **313**, 756–761.

Ullrich,A. *et al.* (1986) *EMBO J.*, **5**, 2503–2512.

von Heijne,G. (1986) *Nucleic Acids Res.*, **14**, 4683–4690.

White,M.F. and Kahn,C.R. (1994) *J. Biol. Chem.*, **269**, 1–4.

White,M.F., Maron,R. and Kahn,C.R. (1985) *Nature*, **318**, 183–186.

White,M.F., Livingston,J.N., Backer,J.M., Lauris,V., Dull,T.J., Ullrich,A. and Kahn,C.R. (1988) *Cell*, **54**, 641–649.

Wieschaus,E. and Nusslein-Volhard,C. (1986) In Roberts,D.B. (ed.), *Drosophila: A Practical Approach.* IRL Press, Oxford, pp. 199–227.

Wilden,P.A., Siddle,K., Haring,E., Backer,J., White,M.F. and Kahn,C.R. (1992) *J. Biol. Chem.*, **267**, 13719–13727.

Yamaguchi,T., Fernandez,R. and Roth,R.A. (1995) *Biochemistry*, **34**, 4962–4968.

Yonezawa,K. *et al.* (1994) *J. Biol. Chem.*, **269**, 4634–4640.

Zhang,B. and Roth,R.A. (1991) *Proc. Natl Acad. Sci. USA*, **88**, 9858–9862.

Zipursky,S.L. and Rubin,G.M. (1994) *Annu. Rev. Neurosci.*, **17**, 373–397.

Received on January 24, 1995; revised on April 19, 1995